Journal of Thermal Analysis and Calorimetry, Vol. 86 (2006) 1, 205–209

THERMAL DECOMPOSITION OF HYDROTALCITE WITH HEXACYANOFERRATE(II) AND HEXACYANOFERRATE(III) ANIONS IN THE INTERLAYER

R. L. Frost, A. W. Musumeci, J. Theo Kloprogge, M. L. Weier, M. O. Adebajo and W. Martens*

Inorganic Materials Research Program, School of Physical and Chemical Sciences, Queensland University of Technology
GPO Box 2434, Brisbane Queensland 4001, Australia

The thermal decompositions of hydrotalcites with hexacyanoferrate(II) and hexacyanoferrate(III) in the interlayer have been studied using thermogravimetry combined with mass spectrometry. X-ray diffraction shows the hydrotalcites have a *d*(003) spacing of 11.1 and 10.9 Å which compares with a *d*-spacing of 7.9 and 7.98 Å for the hydrotalcite with carbonate or sulphate in the interlayer. XRD was also used to determine the products of the thermal decomposition. For the hydrotalcite decomposition the products were MgO, Fe_2O_3 and a spinel $MgAl_2O_4$. Dehydration and dehydroxylation take place in three steps each and the loss of cyanide ions in two steps.

Keywords: *hexacyanoferrate, hydrotalcite, pyroaurite, takovite, thermal analysis*

Introduction

Hydrotalcites, or layered double hydroxides (LDH's) are fundamentally anionic clays, and are less well-known than cationic clays like smectites [1, 2]. The structure of hydrotalcite can be derived from a brucite structure ($Mg(OH)_2$) in which e.g. Al^{3+} or Fe^{3+} (pyroaurite–sjögrenite) substitutes a part of the Mg^{2+} [3–14]. This substitution creates a positive layer charge on the hydroxide layers, which is compensated by interlayer anions or anionic complexes [15, 16]. Further mixtures of these mineral phases with multiple anions in the interlayer are observed. When LDH's are synthesized any appropriate anion can be placed in the interlayer. These anions may be any anion with a suitable negative charge including the hexacyanoferrate(II) and hexacyanoferrate(III) ions [17–19]. The incorporation of these ions has implications in electrochemistry [19–23]. The hydrotalcite may be considered as a gigantic cation which is counterbalanced by anions in the interlayer. In hydrotalcites a broad range of compositions is possible of the type $[M^{2+}_{1-x}M^{3+}_{x}(OH)_2][A^{n-}]_{x/n}\cdot yH_2O$, where M^{2+} and M^{3+} are the di- and trivalent cations in the octahedral positions within the hydroxide layers with *x* normally between 0.17 and 0.33. A^{n-} is an exchangeable interlayer anion [24]. In the hydrotalcites reevesite and pyroaurite, the divalent cations are Ni^{2+} and Mg^{2+}, respectively with the trivalent cation being Fe^{3+}. In these cases, the carbonate anion is the major interlayer counter anion. Of course when synthesizing hydrotalcites any anion may be used [7, 14, 25–27]. Reevesite and pyroaurite are based upon the incorporation of carbonate into the interlayer with *d*(003) spacings of around 8 Å [28, 29]. Normally the hydrotalcite structure based upon takovite (Ni,Al) and hydrotalcite (Mg,Al) has basal spacings of ~8.0 Å where the interlayer anion is carbonate.

Thermal analysis using thermogravimetric techniques enables the mass loss steps, the temperature of the mass loss steps and the mechanism for the mass loss to be determined [6, 11, 30–34]. Thermoanalytical methods provide a measure of the thermal stability of the hydrotalcite. The reason for the potential application of hydrotalcites as catalysts rests with the ability to make mixed metal oxides at the atomic level, rather than at a particle level. Such mixed metal oxides are formed through the thermal decomposition of the hydrotalcite [35, 36]. There are many other important uses of hydrotalcites such as in the removal of environmental hazards in acid mine drainage [37, 38], and a mechanism for the disposal of radioactive wastes [39]. Their ability to exchange anions presents a system for heavy metal removal from contaminated waters [40]. Structural information on different minerals has successfully been obtained recently by sophisticated thermal analysis techniques [6, 30–34]. In this work we report the thermal analysis of hydrotalcite with hexacyanoferrate(II) and hexacyanoferrate(III) in the interlayer.

* Author for correspondence: r.frost@qut.edu.au

1388–6150/$20.00

Akadémiai Kiadó, Budapest, Hungary
Springer, Dordrecht, The Netherlands

Experimental

Synthesis of hydrotalcite compounds

A mixed solution of aluminium and magnesium nitrates ($[Al^{3+}]$=0.25 M and $[Mg^{2+}]$=0.75 M; 1 M=1 mol dm^{-3}) and a mixed solution of sodium hydroxide ($[OH^-]$=2 M) and the desired anion, at the appropriate concentration, were placed in two separate vessels and purged with nitrogen for 20 min (all compounds were dissolved in freshly decarbonated water). The cationic solution was added to the anions via a peristaltic pump at 40 mL min^{-1} and the pH maintained above 9. The mixture was then aged at 75°C for 18 h under a N_2 atmosphere. The resulting precipitate was then filtered thoroughly, with room temperature decarbonated water to remove nitrates and left to dry in a vacuum desiccator for several days. In this way hydrotalcites with different anions in the interlayer were synthesised. The phase composition was checked by X-ray diffraction and the chemical composition by EDXA analyses.

X-ray diffraction

X-ray diffraction patterns were collected using a Philips X'pert wide angle X-ray diffractometer, operating in step scan mode, with CuK_α radiation (1.54052 Å). Patterns were collected in the range 3 to 90° 2θ with a step size of 0.02° and a rate of 30 s per step. Samples were prepared as a finely pressed powder into aluminium sample holders.

Thermal analysis

Thermal decompositions of the hydrotalcites were carried out in a TA® Instruments incorporated high-resolution thermogravimetric analyzer (series Q500) in a flowing nitrogen atmosphere (80 cm^3 min^{-1}). Approximately 50 mg of sample was heated in an open platinum crucible at a rate of 5.0°C min^{-1} up to 1000°C. TG instrument was coupled to a Balzers (Pfeiffer) mass spectrometer for gas analysis. Only selected gases were analyzed.

Results and discussion

X-ray diffraction

The X-ray diffraction patterns for the hexacyanoferrate(II) and hexacyanoferrate(III) interlayered hydrotalcites are shown in Fig. 1. For comparison the XRD patterns of the sulphate and carbonate interlayered hydrotalcite are shown. The XRD patterns clearly show the formation of the hydrotalcites with the different anions in the interlayer. The XRD patterns also show no impurities in the synthesised hydrotalcites. Hydrotalcite

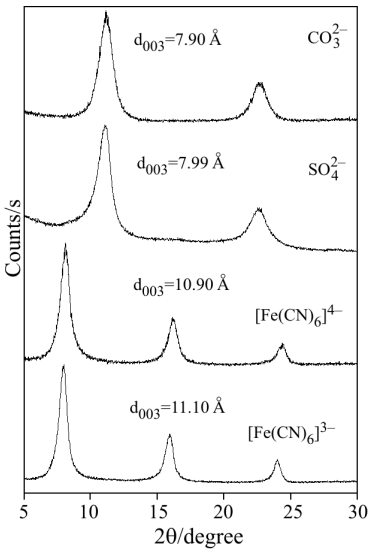

Fig. 1 X-ray diffraction patterns of hydrotalcite with carbonate, sulphate, hexacyanoferrate(II) and hexacyanoferrate(III) anions in the interlayer

normally has a *d*(003) spacing of 7.9 Å. The sulphate interlayered hydrotalcite has a spacing of 7.99 Å. The hexacyanoferrate(II) complex has a spacing of 10.9 Å and the hexacyanoferrate(III) hydrotalcite 11.1 Å. The increased interlayer spacing is due to the size of the anion between the brucite-like layers.

Thermogravimetry and mass spectrometric analysis of the hexacyanoferrate(II)–hydrotalcite

The thermal analysis patterns for the hexacyanoferrate(II) interlayered hydrotalcite are shown in Fig. 2. The ion current curves are displayed in Fig. 3. A significant number of mass loss steps are observed. These occur at 89, 157, 270, 354, 413 and 460°C. The total mass loss for the steps at 89 and 157°C is 16%.

The ion current curves show that water is lost over the 50 to 200°C temperature range. The CN units are lost in two steps at 259 and 416°C. Some carbon dioxide is also lost at 415 and 460°C. The presence of

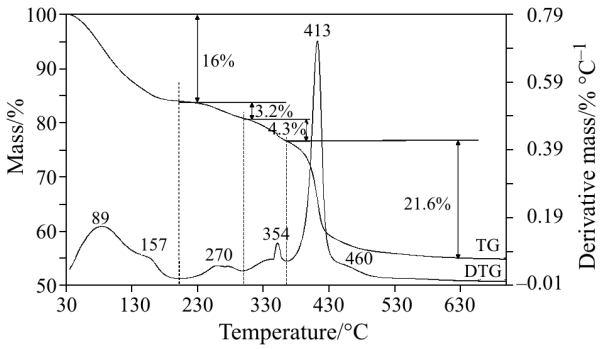

Fig. 2 TG and DTG of the thermal decomposition of hexacyanoferrate(II) interlayered hydrotalcite

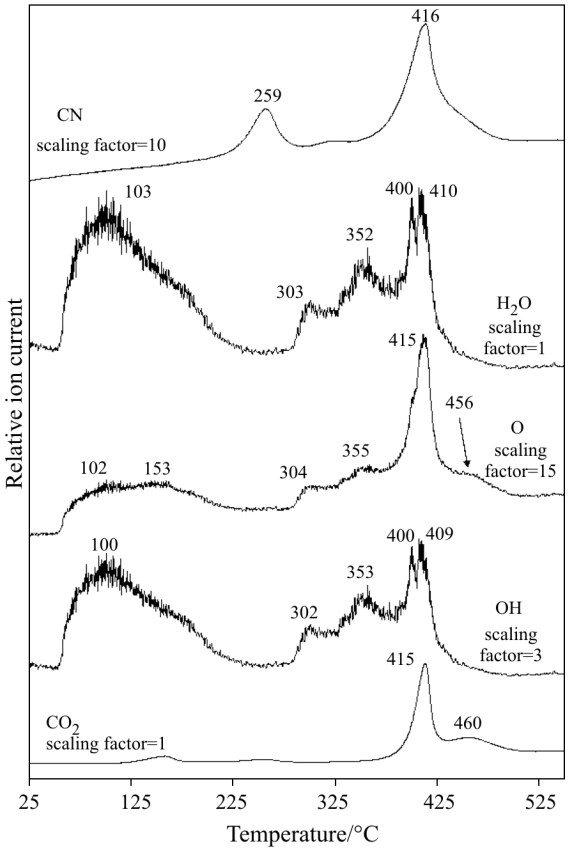

Fig. 3 Relative ion current curves for the thermal decomposition of hexacyanoferrate(II) interlayered hydrotalcite

carbon dioxide is an impurity in the experiment and despite all the efforts to keep the carbon dioxide out of the system, some still enters the hydrotalcite interlayer. The ion current curves also show that water vapour is evolved at 303, 352, 404 and 409°C. This water is the result of the dehydroxylation of the hydrotalcite. It is noteworthy that the ion current curves show four distinct dehydroxylation steps. In comparison, the DTG shows an overlapping profile of mass losses without these distinguishing features. The DTG curve is dominated by the mass loss associated with the removal of the CN units. The theoretical total mass loss for the hexacyanoferrate(II)–interlayered hydrotalcite based upon the formula $Mg_6Al_2(OH)_{16}(Fe(CN)_6)_{0.5}\cdot 7H_2O$ is 49.5%. The total mass loss determined experimentally is 45.0%. The mass loss of 16.0% over the 50 to 200°C temperature range is attributed to the process of dehydration of the hydrotalcite. Two mass loss steps are observed at 270 and 354°C. The first mass loss step is ascribed to the loss of CN units and to some OH units. This step represents the first dehydroxylation step. The major mass loss step is at 413°C with a loss of 21.6%. Associated with this mass loss is the loss of OH units and CO_2 impurities.

Mechanism for the decomposition of hydrotalcite with hexacyanoferrate(II) in the interlayer

The following steps describe the thermal decomposition of the hexacyanoferrate(II)–interlayered hydrotalcite.

Step 1 at 89°C

This step includes the loss of adsorbed water.

$$Mg_6Al_2(OH)_{16}(Fe(CN)_6)_{0.5}\cdot 7H_2O\rightarrow$$

$$Mg_6Al_2(OH)_{16}(Fe(CN)_6)_{0.5}\cdot 2H_2O+5H_2O$$

This step represents the first dehydration step and shows five moles of water are lost at this temperature.

Step 2 at 157°C

$$Mg_6Al_2(OH)_{16}(Fe(CN)_6)_{0.5}\cdot 2H_2O\rightarrow$$

$$Mg_6Al_2(OH)_{16}(Fe(CN)_6)_{0.5}+2H_2O$$

This step represents the second dehydration step and shows two moles of water are lost at this temperature.

Step 3 at 270°C

$$Mg_6Al_2(OH)_{16}(Fe(CN)_6)_{0.5}\rightarrow$$

$$Mg_6Al_2O_2(OH)_{13}Fe(CN)_4)_{0.5}+HCN+H_2O$$

This step shows the first loss of OH units together with some CN units probably as HCN.

Step 4 at 354°C

$$Mg_6Al_2O_2(OH)_{13}(Fe(CN)_4)_{0.5}\rightarrow$$

$$Mg_6Al_2O_3(OH)_{11}(Fe(CN)_4)_{0.5}+H_2O$$

This step represents a second dehydroxylation step.

Step 5 at 452 and at 460°C

$$2Mg_6Al_2O_3(OH)_{11}(Fe(CN)_4)_{0.5}\rightarrow$$

$$12MgO+2Al_2O_3+FeO+4HCN+9H_2O$$

Thermogravimetry and mass spectrometric analysis of the hexacyanoferrate(III)–hydrotalcite

TG analysis pattern for the hexacyanoferrate(III) interlayered hydrotalcite shows a simpler profile than for the hexacyanoferrate(II) interlayered hydrotalcite (Fig. 4). The DTG pattern shows three mass loss steps in the 50 to 200°C temperature range at around 345 and 414°C. The first mass loss step is associated with dehydration, the second mass loss step with dehydroxylation and the third mass loss step with loss of the CN units and also the loss of the additional OH units.

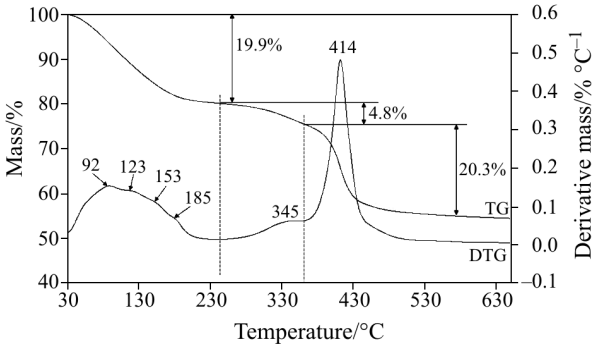

Fig. 4 TG and DTG of the thermal decomposition of hexacyanoferrate(III) interlayered hydrotalcite

The ion current curves for the evolved gases are shown in Fig. 5. The theoretical mass loss for the dehydration step based upon the formula $Mg_6Al_2(OH)_{16}(Fe(CN)_6)_{0.66}.4H_2O$ is 11.1%. The experimental mass loss is 19.9%. This value corresponds well with 7 moles of water in the formula. In other words, the correct formula for the hexacyanoferrate(III) hydrotalcite is $Mg_6Al_2(OH)_{16}(Fe(CN)_6)_{0.66}.7H_2O$. The mineral honnessite can exist in two forms honnessite with 4 moles of water in the formula and hydrohonnessite with 7 moles of water in the formula. The total mass loss for the loss of OH units for the hydrotalcite

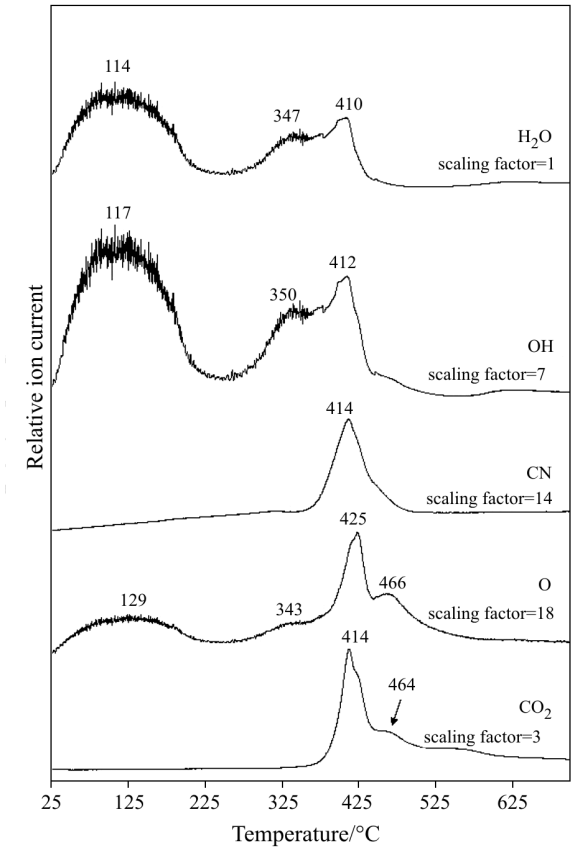

Fig. 5 Relative ion current curves for the thermal decomposition of hexacyanoferrate(III) interlayered hydrotalcite

$Mg_6Al_2(OH)_{16}(Fe(CN)_6)_{0.66}.7H_2O$ is 22.2%. The theoretical mass loss for the CN units is 12.03%. The experimental mass loss for the two steps at 345 and 414°C is 25.1% which is low compared with the theoretical total loss of 34.2%.

Mechanism for the decomposition of hydrotalcite with hexacyanoferrate(III) in the interlayer

The following steps describe the thermal decomposition of the hexacyanoferrate(III)–interlayered hydrotalcite.

Step 1 from 50 to 200°C

This step includes the loss of adsorbed water.

$$Mg_6Al_2(OH)_{16}(Fe(CN)_6)_{0.66}.7H_2O\rightarrow$$

$$Mg_6Al_2(OH)_{16}(Fe(CN)_6)_{0.66}+7H_2O$$

DTG pattern shows a number of overlapping steps at 92, 123, 153 and 185°C. Each of these steps is attributed to dehydroxylation. Calculations show seven moles of water are lost at this temperature.

Step 2 at 345°C

$$Mg_6Al_2(OH)_{16}(Fe(CN)_6)_{0.66}\rightarrow$$

$$Mg_6Al_2O_2(OH)_{12}Fe(CN)_6)_{0.66}+2H_2O$$

This step represents a dehydroxylation step. Calculations show approximately 25% of the OH units is lost at this temperature.

Step 3 at 414°C

$$Mg_6Al_2O_2(OH)_{12}Fe(CN)_6)_{0.66}\rightarrow$$

$$(6MgO)Al_2O_3(Fe_2O_3)_{0.33}+4H_2O+4HCN$$

This step represents the third dehydroxylation step and 12 OH units are lost at this temperature. Simultaneously 4 moles of CN units are lost.

Conclusions

The thermal decomposition of hydrotalcites based upon a Mg/Al ratio of 6/2 with hexacyanoferrate(II) and (III) in the interlayer has been studied using thermal analysis techniques complimented with X-ray diffraction. The products of the thermal decomposition were a mixture of oxides and a spinel. Three processes are observed in the thermal decomposition firstly dehydration, secondly dehydroxylation and loss of the cyanide ions. Dehydration and dehydroxylation takes place in several steps. Mechanisms were proposed for each of the steps in the thermal decomposition.

Acknowledgements

The financial and infra-structure support of the Queensland University of Technology Inorganic Materials Research Program of the School of Physical and Chemical Sciences is gratefully acknowledged. The Australian Research Council (ARC) is thanked for funding the thermal analysis facility.

References

1 K. Hashi, S. Kikkawa and M. Koizumi, Clays Clay Miner., 31 (1983) 152.
2 L. Ingram and H. F. W. Taylor, Mineral. Magazine J. Mineral. Soc., (1876–1968) 36 (1967) 465.
3 J. T. Kloprogge, L. Hickey and R. L. Frost, Mater. Chem. Phys., 89 (2005) 99.
4 R. L. Frost and K. L. Erickson, Spectrochim. Acta, Part A, 61 (2005) 51.
5 K. L. Erickson, T. E. Bostrom and R. L. Frost, Mater. Lett., 59 (2004) 226.
6 R. L. Frost and K. L. Erickson, J. Therm. Anal. Cal., 76 (2004) 217.
7 R. L. Frost and K. L. Erickson, Thermochim. Acta, 421 (2004) 51.
8 J. T. Kloprogge, L. Hickey and R. L. Frost, J. Raman Spectrosc., 35 (2004) 967.
9 J. T. Kloprogge, L. Hickey and R. L. Frost, J. Solid State Chem., 177 (2004) 4047.
10 R. L. Frost and Z. Ding, Thermochim. Acta, 405 (2003) 207.
11 R. L. Frost, W. Martens, Z. Ding and J. T. Kloprogge, J. Therm. Anal. Cal., 71 (2003) 429.
12 R. L. Frost, M. L. Weier, M. E. Clissold and P. A. Williams, Spectrochim. Acta, Part A, 59 (2003) 3313.
13 R. L. Frost, M. L. Weier, M. E. Clissold, P. A. Williams and J. T. Kloprogge, Thermochim. Acta, 407 (2003) 1.
14 R. L. Frost, M. L. Weier and J. T. Kloprogge, J. Raman Spectrosc., 34 (2003) 760.
15 R. M. Taylor, Clay Mineral., 17 (1982) 369.
16 H. F. W. Taylor, Mineral. Magazine J. Mineral. Soc., (1876–1968) 37 (1969) 338.
17 I. Crespo, C. Barriga, V. Rives and M. A. Ulibarri, Solid State Ionics, 101–103 (1997) 729.
18 I. Crespo, C. Barriga, M. A. Ulibarri, G. Gonzalez-Bandera, P. Malet and V. Rives, Chem. Mater., 13 (2001) 1518.
19 K. Okada, F. Matsushita, S. Hayashi and A. Yasumori, Clay Sci., 10 (1996) 1.
20 K. Itaya, H. C. Chang and I. Uchida, Inorg. Chem., 26 (1987) 624.
21 B. R. Shaw, Y. Deng, F. E. Strillacci, K. A. Carrado and M. G. Fessehaie, J. Electrochem. Soc., 137 (1990) 3136.
22 K. Yao, M. Taniguchi, M. Nakata and A. Yamagishi, J. Electroanal. Chem., 458 (1998) 249.
23 K. Yao, M. Taniguchi, M. Nakata, M. Takahashi and A. Yamagishi, Langmuir, 14 (1998) 2890.
24 H. C. B. Hansen and C. B. Koch, Appl. Clay Sci., 10 (1995) 5.
25 J. T. Kloprogge, J. Kristof and R. L. Frost, 2001 a Clay Odyssey, Proceedings of the International Clay Conference, 12th, Bahia Blanca, Argentina, July 22–28, 2001 (2003) 451.
26 R. L. Frost, M. L. Weier, M. E. Clissold and P. A. Williams, Spectrochim. Acta, Part A, 59 (2003) 3313.
27 R. L. Frost, M. L. Weier, M. E. Clissold and P. A. Williams, Spectrochim. Acta, Part A, 59 (2003) 3313.
28 D. L. Bish and A. Livingstone, Mineral. Magazine, 44 (1981) 339.
29 E. H. Nickel and R. M. Clarke, Am. Mineral., 61 (1976) 366.
30 E. Horváth, J. Kristóf, R. L. Frost, N. Heider and V. Vágvölgyi, J. Therm. Anal. Cal., 78 (2004) 687.
31 R. L. Frost, M. L. Weier and K. L. Erickson, J. Therm. Anal. Cal., 76 (2004) 1025.
32 R. L. Frost and K. L. Erickson, J. Therm. Anal. Cal., 78 (2004) 367.
33 E. Horváth, J. Kristóf, R. L. Frost, A. Rédey, V. Vágvölgyi and T. Cseh, J. Therm. Anal. Cal., 71 (2003) 707.
34 J. Kristóf, R. L. Frost, J. T. Kloprogge, E. Horváth and E. Makó, J. Therm. Anal. Cal., 69 (2002) 77.
35 F. Rey, V. Fornes and J. M. Rojo, J. Chem. Soc., Faraday Trans., 88 (1992) 2233.
36 M. Valcheva-Traykova, N. Davidova and A. Weiss, J. Mater. Sci., 28 (1993) 2157.
37 G. Lichti and J. Mulcahy, Chem. Aust., 65 (1998) 10.
38 Y. Seida and Y. Nakano, J. Chem. Eng. Jpn., 34 (2001) 906.
39 Y. Roh, S. Y. Lee, M. P. Elless and J. E. Foss, Clays Clay Mineral., 48 (2000) 266.
40 Y. Seida, Y. Nakano and Y. Nakamura, Water Res., 35 (2001) 2341.

Received: August 2, 2005
Accepted: July 20, 2006

DOI: 10.1007/s10973-005-6933-z